

Heterogeneous Photocatalytic Degradation of Disulfoton in Aqueous TiO₂ Suspensions: Parameter and Reaction Pathway Investigations

Ming-Hung Chen,^a Chiing-Chang Chen,^b Ren-Jang Wu^a and Chung-Shin Lu^{c*}

^aDepartment of Applied Chemistry, Providence University, Taichung 433, Taiwan, ROC

^bDepartment of Science Application and Dissemination, National Taichung University of Education, Taichung 403, Taiwan, ROC

^cDepartment of General Education, National Taichung University of Science and Technology, Taichung 403, Taiwan, ROC

(Received: Jan. 17, 2012; Accepted: Jul. 31, 2012; Published Online: Jan. 17, 2013; DOI: 10.1002/jccs.201200027)

The photocatalytic degradation of organophosphorus insecticide disulfoton is investigated by having titanium dioxide (TiO₂) as a photocatalyst. About 99% of disulfoton is degraded after UV irradiation for 90 min. The effects of the solution pH, catalyst dosage, light intensity, and inorganic ions on the photocatalytic degradation of disulfoton are also investigated, as well as the reaction intermediates which are formed during the treatment. Eight intermediates have been identified and characterized through a mass spectra analysis, giving insight into the early steps of the degradation process. To the best of our knowledge, this is the first study reporting the degradation pathways of disulfoton. The results suggest that possible transformation pathways may involve in either direct electron or hole transfer to the organic substrate. The photodegradation of disulfoton by UV/TiO₂ exhibits pseudo-first-order reaction kinetics and a reaction quantum yield of 0.267. The electrical energy consumption per order of magnitude for photocatalytic degradation of disulfoton is 85 kWh/(m³ order).

Keywords: Photocatalysis; Titanium dioxide; Disulfoton; Intermediate.

INTRODUCTION

Organophosphorus pesticides (OPs) are popular candidates to replace the more persistent organochlorine compounds which are suspected to be bioaccumulated up the food chain. OPs represent more than one-third of the total insecticides used in the world.^{1,2} The primary acute toxic effect caused by organophosphorus pesticides is usually the inhibition of enzyme acetylcholinesterase, which plays a critical role in the proper functioning of nerve cells.^{3,4} OPs act as the cholinesterase inhibitors in insects and mammals and bring about a non-reversible phosphorylation of esterases in the organisms' central nervous system. This activity is also responsible for the toxicity in humans.^{5,6} Due to their extensive use, they are the chemicals most frequently associated with toxicity to aquatic fauna as well as humans.⁷ Disulfoton is a thioether-containing organophosphate pesticide that is found widely used in agriculture, primarily on crops such as corn, potatoes, cotton and grains. Its chemical structure is shown in Fig. 1. About 1.2 million pounds of disulfoton are used annually in the United States.⁸ Contamination of the environment by disulfoton is primarily due to the release during its use as insecticide by constant leaching and superficial runoff during rainfall. As a

result, effective purification methods for removing these pollutants from water are in urgent demand.

There are several methods to remove OPs from water, including adsorption,⁹ chemical oxidation,¹⁰ hydrolysis¹¹ and biodegradation.¹² Each method has its own limitations and disadvantages in applications. Adsorption is one of the most recognized methods used in the removal of such hazardous substances from polluted water.¹³ Adsorption involves only in phase transfer of pollutants and decreasing their concentration from water without degradation;¹⁴ the chemical oxidation method is unable to mineralize all organic substances; hydrolysis processes are typically very slow and sometimes inefficiency; and in biological treatment methods, the slow reaction rates and the disposal of activated sludge are the drawbacks to be considered.^{15,16}

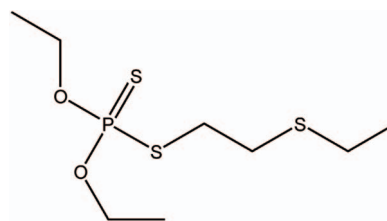
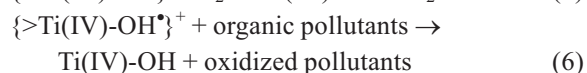
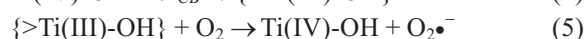
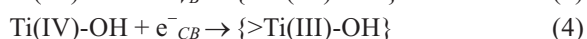
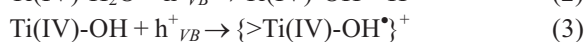
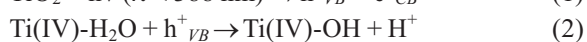
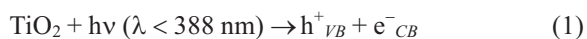


Fig. 1. Chemical structure of disulfoton.

* Corresponding author. Tel: +886-4-2219-6999; Fax: +886-4-2219-6825; E-mail: cslu6@nutc.edu.tw

The processes involving in light and homogeneous photochemistry have been interested in the last years because they overcame the above disadvantage. Advanced oxidation processes (AOPs), based on H₂O₂/UV, O₃/UV, and H₂O₂/O₃/UV combinations, employing photolysis of H₂O₂ and ozone which produce hydroxyl radicals ($\cdot\text{OH}$) have grown success. Hydroxyl radical is strongly oxidative ($E^0 = 2.8 \text{ V}$)¹⁵ that it can destroy hazardous contaminants. The end products are carbon dioxide, water and inorganic mineral salts.¹⁷⁻¹⁹ Homogeneous photochemistry, in general, requires high energy photons and rarely enhances the total degradation of the pollutant.

Photocatalytic oxidation using semiconductor materials, such as TiO₂, has been demonstrated as the effective means for organic degradation in a very short time and with high efficiency.^{17,20} TiO₂ is broadly used as a photocatalyst because of its non-toxicity, photochemical stability and low cost.²¹ When activation of the semiconductor photocatalyst for reaction is achieved through the absorption of photon of ultra-bandgap energy (E_g), electron is promoted from the lowest unoccupied energy band (the valence band, h^+_{VB}) to the conduction band, with the concomitant generation of hole in the highest occupied band (the conduction band, e^-_{CB}), as set forth in equation (1). OH radicals were formed directly by the oxidation of H₂O with holes in the valence band of TiO₂, which are shown in equation (2)-(3). The processes are described by equation (4)-(5), the surface trapped CB electron could reduce the organic substrate or react with the adsorbed molecular O₂, generation of the superoxide radical anion, O₂ \cdot^- . The hydroxyl radical is a powerful oxidizing agent and attacks organic pollutants presented at or near the surface of TiO₂, as shown in equation (6).^{15,21-23}



where $>\text{TiOH}$ represents the primary hydrated surface functionality of TiO₂, e^-_{CB} is a conduction band electron, h^+_{VB} is the valence band hole, $\{>\text{Ti(IV)-OH}^+\}^+$ is the surface trapped VB hole (surface bound hydroxyl radical, $\cdot\text{OH}$), and $\{>\text{Ti(III)-OH}\}$ is the surface trapped CB elec-

tron.

Little has been reported on the degradation of disulfoton under UV irradiation. Zamy et al.²⁴ investigated the photochemical transformation of four selected organophosphorus pesticides (disulfoton, isofenfos, isazofos and profenfos) in dilute aqueous solutions. They analyzed the degradation products of disulfoton upon polychromatic irradiation ($\lambda > 285 \text{ nm}$) in aqueous solution. Their results showed the formation of disulfoton-oxon, disulfoton-sulfoxide and dithiophosphoric acid-O, S, O-triethylester. Elsewhere, Hebert and Miller²⁵ studied the photolysis of disulfoton on soil. They attributed the degradation of disulfoton to the generation of singlet oxygen, but no information concerning degradation products was being made available.

To the best of our knowledge, no studies on the photocatalytic degradation of disulfoton have been published yet. In this paper, the photocatalytic degradation of disulfoton is reported for the first time. Various parameters which might affect the photodegradation of disulfoton in the presence of TiO₂ suspensions are investigated in order to obtain a more complete knowledge of TiO₂ photocatalysis. This study also focuses on the identification of the reaction intermediates and the understanding of the mechanistic details of the photodegradation of disulfoton in the TiO₂/UV light process as a foundation for future application of this energy saving technology.

EXPERIMENTAL SECTION

Materials and reagents

Disulfoton (98.2%) was obtained from Sigma-Aldrich. Standard solution containing 5 mg L⁻¹ of disulfoton in water was prepared, protected from light, and stored at 4 °C. 1,2-diethyl-disulfane (Sigma-Aldrich) was used for intermediate confirmation. Other chemicals were of reagent grade and used as such without further purification. Titanium dioxide (P25)—a known mixture of 80% anatase and 20% rutile, with an average particle size of 30 nm, nonporous, and a reactive surface area of $50 \pm 10 \text{ m}^2 \text{ g}^{-1}$ —was used as received for all degradation experiments and supplied by Degussa Co. De-ionized water was used throughout this study. The water was purified with a Milli-Q water ion-exchange system (Millipore Co.) to give a resistivity of $1.8 \times 10^7 \Omega\text{-cm}$.

Apparatus and instruments

The schematic diagram of experimental apparatus was shown in our early report.²⁶ The C-75 Chromato-Vue cabinet of UVP provided a wide area of illumination from the 15-Watt UV-365 nm tubes positioned on two sides of the cabinet interior.

Solid-phase microextraction (SPME) was utilized for the analysis of disulfoton and intermediates resulting from the photocatalytic degradation process. SPME holder and fiber-coating divinylbenzene-carboxen-polydimethylsiloxane (DVB-CAR-PDMS 50/30 μm) were supplied from Supelco (Bellefonte, PA). GC/MS analyses were run on a Perkin-Elmer AutoSystem-XL gas chromatograph interfaced to a TurboMass selective mass detector. The analysis of ionic byproducts was performed by ion chromatography (IC) with a Dionex ICS-90 instrument.

Procedures and analysis

Disulfoton solution (5 mg L^{-1}) with the appropriate amount of photocatalyst was mixed and used in photocatalytic experiments. For reactions in different pH media, the initial pH of the suspensions was adjusted by adding a few drops of either 0.1 N NaOH or 0.1 N HNO₃ solutions. Prior to irradiation, the dispersion was magnetically stirred in the dark for 30 min to ensure the establishment of the adsorption/desorption equilibrium. Irradiation was carried out using two UV-365 nm lamps (15 watt). After each irradiation cycle, the amount of disulfoton was thus determined by SPME-GC/MS. The aqueous TiO₂ dispersion was sampled (5 mL) and centrifuged to separate the TiO₂ particles. The clear solution was then transferred into 4 mL sample vial. The SPME fiber was directly immersed into the sample solution to extract disulfoton and its intermediates for 30 min at room temperature, with magnetic stirring at $550 \pm 10 \text{ rpm}$ on the Corning stirrer/plate (Corning, USA). Finally, the compounds were thermally desorbed from the fiber to the GC injector for 40 min. Separation was carried out in a DB-5 capillary column (5% diphenyl/95% dimethyl-siloxane), 60 m, 0.25-mm i.d., and 1.0- μm thick film. A split-splitless injector was used under the conditions of injector temperature 250 °C, a split ratio 1:10, the helium carrier gas flow 0.6 mL/min, the oven temperature program 1.0 min at 60 °C then being increased at $8 \text{ }^\circ\text{C min}^{-1}$ until reaching 240 °C, which was kept for 16.5 min. The total run time was 40 min.

Mass spectrometric detection was performed in full-scan conditions for both electron impact (EI) and chemical ionization (CI) using isobutane as reagent gas. The ion source and inlet line temperatures were set at 220 and 250 °C, respectively. Electron impact mass spectra were obtained at 70 eV of electron energy and monitored from 10 to 350 m/z . The mass spectrometer was tuned regularly with perfluorotributylamine using the fragment ions at m/z 69, 131, 219 and 502. EI mass spectra were identified using the NIST 2008 Library, and the analytes were automatically identified by the NIST MS-Search 2.0 software. Chemical ionization mass spectrometry was operated in the positive ionization mode, isobutane was used as reagent gas at an apparent pressure of 4.4×10^{-4} Torr in the ionization source. The full scan mode with

a mass range of m/z 40–350 was used to confirm the analytes. The autotuning software performed the reagent gas flow adjustment and the lens and electronic tuning.

The ionic byproducts from disulfoton degradation were analyzed using a Dionex ICS-90 ion chromatograph. The column was an IonPac® AS4A-SC (4 \times 250 mm) for phosphate (PO_4^{3-}) and sulfate (SO_4^{2-}) analyses. The flow rate was 1.0 mL/min, and the injection volume was 100 μL for the filtered reaction samples. The eluent consisted of a mixture of 3.5 mM Na₂CO₃ and 1 mM NaHCO₃ for the anion analysis. For these operating conditions, the retention time for PO_4^{3-} and SO_4^{2-} was 5.4 and 6.7 min, respectively. For quantitative studies, standard solutions and calibration curves for each ion were prepared in the range from 1 to 10 mg L⁻¹. In order to avoid adsorbed processes of the anions on the surface of the catalyst during the reaction progress, a desorption procedure was applied. This consisted of the addition of NaOH (1 N) to the reaction mixture after irradiation until it reached a pH of 12.

RESULTS AND DISCUSSION

Photodegradation kinetics

Regression analysis based on the pseudo-first-order reaction kinetics for the degradation of disulfoton in photocatalytic process was conducted and the results are shown in Fig. 2. Degradation rate constants (k_{app}) were determined from the slope of $\ln C_0/C = k_{\text{app}}t$ plots. About 99% of the disulfoton was degraded after UV irradiation for 90 min. Table 1 lists the calculated values of k_{app} and the linear regression coefficients for the pseudo-first-order kinetics of the photodegradation of the studied compound. It seemed that the photocatalytic degradation of disulfoton followed pseudo-first-order kinetics satisfactorily. Similar results were reported by others for the photocatalytic degradation of organophosphorus pesticides (Table 2). The disulfoton reaction rate is similar to other organophosphorus com-

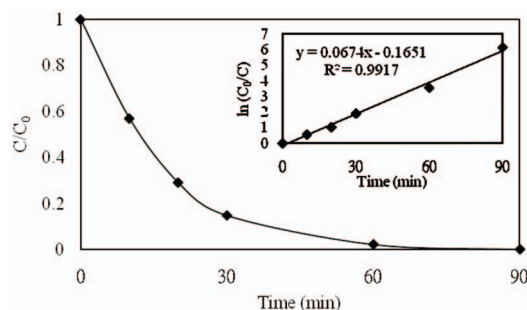


Fig. 2. Photodegradation kinetics of disulfoton in the presence of TiO₂ particles. Experimental condition: disulfoton concentration 5 mg L^{-1} , TiO₂ concentration 0.5 g L^{-1} , pH 6.

Table 1. Photodegradation kinetics parameters (rate constants and linear regression coefficients R^2) for disulfoton in the presence of TiO₂ (0.5 g L⁻¹)

pH	K_{app} (min ⁻¹)	R^2
4	0.0309	0.9963
6	0.0674	0.9917
9	0.0799	0.9939

pounds treated by TiO₂ photocatalysis.

pH effect

Control experiments were performed to guarantee that the results obtained during the photocatalytic tests were consistent and not due to hydrolysis. The results indicated that only slight hydrolysis was detected after 3 h in the solution kept in the dark at pH 6 (see Fig. 3). Photocatalytic degradation of disulfoton by TiO₂ obtained in this study was much faster than it by hydrolysis. The contribution of hydrolysis is negligible.

The real effluent stuff of pesticide could be discharged at a different pH,²⁷ and therefore the effect of pH on the rate of photocatalytic degradation of disulfoton was studied. The results indicated that the degradation rate increased with an increase in pH in the studied range of 4–11 (Fig. 3). The effect of pH on a photocatalytic reaction is

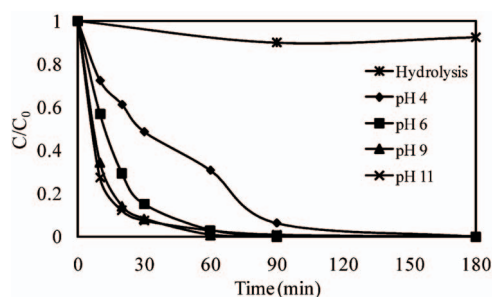


Fig. 3. pH effect on the photodegradation rate of disulfoton with concentration of TiO₂ at 0.5 g L⁻¹ and disulfoton at 5 mg L⁻¹.

generally ascribed to the surface charge of the photocatalyst and its relation to the ionic form of the organic compound (anionic or cationic). Electrostatic attraction or repulsion between the photocatalyst's surface and the organic molecule took place, and these events consequently enhanced or inhibited, respectively, the photodegradation rate.^{27,28} Due to the non-ionic property of disulfoton, the observed increase of the degradation rate with an increase in pH could be ascribed to the generation of hydroxyl radicals through photo-oxidation by photocatalyst's surface holes due to the presence of a large quantity of OH⁻ ions. Consequently, a higher concentration of [•]OH species was formed, and the overall rate was enhanced, as indicated in equation (3).

Effect of TiO₂ dosage

For economic removal of pesticide effluent from wastewater, it is necessary to find the optimum amount of catalyst for efficient degradation. Hence, the effect of TiO₂ dosage on the photodegradation rate of disulfoton was investigated using TiO₂ at different concentrations, keeping all other parameters identical. The optimum amount expressed in g_{cat} per L of solution was found equal to 0.5 g L⁻¹, and the result is shown in Fig. 4. The degradation rate was found to increase with increasing TiO₂ concentration up to a certain

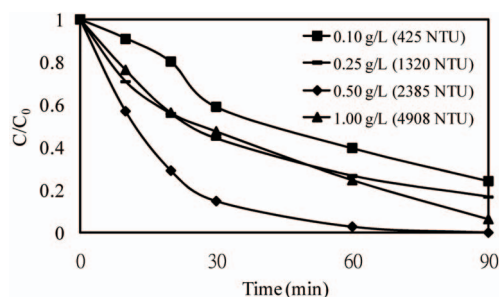


Fig. 4. Effect of TiO₂ dosage on the photodegradation rate of disulfoton. Experimental condition: disulfoton concentration 5 mg L⁻¹, pH 6.

Table 2. Photodegradation kinetics parameters (rate constants and linear regression coefficients R^2) for other organophosphorus pesticides in the presence of TiO₂

OPs concentration	TiO ₂ dosage (g L ⁻¹)	pH value	K_{app} (min ⁻¹)	R^2	Ref
Parathion (5 mg L ⁻¹)	1.0	6.5	0.167	0.998	18
Phorate (12 mg L ⁻¹)	0.5	6	0.1020	0.996	19
Terbufos (5 mg L ⁻¹)	0.5	6	0.0814	0.985	26
Dichlorvos (20 mg L ⁻¹)	0.1	-	0.103	0.981	40
Dimethoate (20 mg L ⁻¹)	0.1	-	0.048	0.976	40
Disulfoton (5 mg L ⁻¹)	0.5	6	0.0674	0.9917	this study

value and then obviously decrease at high TiO_2 dosages. The activity of photocatalyst could be attributed to the availability of active sites on catalyst surface when the light penetration being in the suspension. The active sites of catalyst surface increased with the catalyst concentration in the suspension. However, when TiO_2 was overdosed, the intensity of incident UV light was attenuated because of the shielded of incident light by TiO_2 particle and increased turbidity of the suspension reducing the light transmission. Furthermore, the increase of light scattering which counteracted the positive effect came from the dosage increment and therefore reduced the overall performance.

The solution turbidity measured using HACH 2100P Turbidimeter was ca. 425, 1320, 2385 and 4908 NTU for the solution with different concentrations of TiO_2 (0.1, 0.25, 0.5 and 1.0 g/L), respectively. The excess of catalyst concentration might increase the turbidity of the solutions leading to a shielding effect on the penetration of UV light and inducing an unfavorable condition for the photocatalytic degradation of disulfoton. The kinetics of disulfoton disappearance in the presence of different concentrations of TiO_2 (0.1, 0.25, 0.5 and 1.0 g/L) followed an apparent first-order degradation curve which is consistent to the Langmuir–Hinshelwood model. The k_{app} values in the presence of 0.1, 0.25, 0.5 and 1.0 g/L of TiO_2 were 0.016, 0.0189, 0.0674 and 0.0285 min^{-1} , respectively, confirming the positive influence of the increased number of TiO_2 active sites on the process kinetics. However, this beneficial effect tends to level off and then to decrease for TiO_2 concentrations higher than 1.0 g/L depending on the reactor, due to relevant scattering of the incident light.²⁹ Similar observations were reported by other authors as well.^{30,31} All further studies were made using a TiO_2 dosage of 0.5 g L^{-1} .

Effect of light intensity

UV light intensity is an important factor in the process of photocatalytic degradation. The effect of light intensity was studied, keeping the wavelength (365 nm) unaltered. The effect of the UV light intensity on the degradation of disulfoton is illustrated in Fig. 5. The results indicated that the degradation rate increases with increase in the light intensity. It might be because a higher UV intensity provided more photons to activate TiO_2 thus generating more $\cdot\text{OH}$ for disulfoton degradation.

Effects of anions

The study of the effects of anions on the photocatalytic degradation of disulfoton is important because anions are rather common in natural water and industrial waste-

water. The effects of Cl^- and NO_3^- ions on the degradation rate of disulfoton were examined individually by adding NaCl and NaNO_3 to the system until the resultant solution contained 0.05 M of Cl^- and NO_3^- ions before the irradiation began. The degradation rate was inhibited in the presence of Cl^- and NO_3^- ions as shown in Fig. 6. To investigate the effect of variation of the concentration of anion on the degradation rate of disulfoton, nitrate was also added at a different concentration (0.1 M) in the initial solution. It can be seen that the photodegradation efficiency of disulfoton decreases further with increasing the concentration of anion. This might be because of the following two reasons. (i) The adsorbed anions might compete with disulfoton for the active sites on the TiO_2 surface or deactivate the photocatalyst and, subsequently, slow down the degradation rate of disulfoton molecule. (ii) The reaction of positive holes (h^+) and hydroxyl radical ($\cdot\text{OH}$) with anions that behaved as h^+ and $\cdot\text{OH}$ scavengers resulted in prolonged disulfoton removal. A major drawback resulting from the high reactivity and non-selectivity of $\cdot\text{OH}$ was that it also reacted with non-target substances present in the background water matrix, i.e. inorganic anions present in water. This result in a

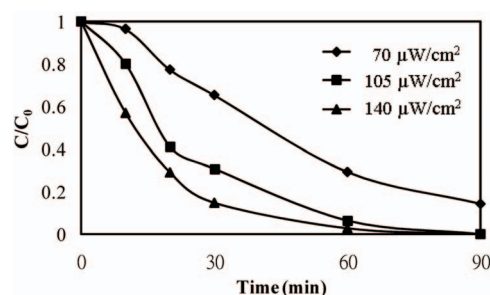


Fig. 5. Effect of light intensity on the photocatalytic degradation of disulfoton in water. Experimental condition: disulfoton concentration 5 mg L^{-1} , TiO_2 concentration 0.5 g L^{-1} , pH 6.

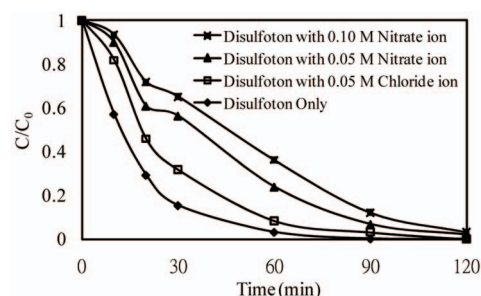


Fig. 6. Effect of anions on the photocatalytic degradation of disulfoton in water. Experimental condition: disulfoton concentration 5 mg L^{-1} , TiO_2 concentration 0.5 g L^{-1} , pH 6.

higher $\cdot\text{OH}$ demanded to accomplish the desired degree of degradation.³²⁻³⁴ The decrease in rate was higher in the presence of NO_3^- than that of Cl^- ions. It might be because nitrate had a larger anionic size than chloride did, which could block the active sites more effectively.³⁵

Effects of cations

The degradation of disulfoton was studied in the presence of 0.05 M solutions of $\text{Fe}(\text{NO}_3)_3$ and $\text{Cu}(\text{NO}_3)_2$. It was found that the degradation of disulfoton in the presence of these concentrations of $\text{Fe}(\text{NO}_3)_3$ and $\text{Cu}(\text{NO}_3)_2$ decreased. That is, the degradations of disulfoton in the presence of $\text{Fe}(\text{NO}_3)_3$ and $\text{Cu}(\text{NO}_3)_2$ were 87.6% and 57.2%, respectively, as against 99% in their absence, as shown in Fig. 7.

Formation of ionic by-products

Since disulfoton is a phosphorodithioate pesticide containing sulfur and phosphorus atoms, the sulfate (SO_4^{2-}) and phosphate (PO_4^{3-}) are potential ionic degradation by-products. Measurements of phosphate and sulfate ions gave valuable information about how this process was achieved. Therefore, the ionic by-products produced during photocatalysis were measured. Preliminary results showed that PO_4^{3-} was retained on the surface of TiO_2 in the degradative process and this ion was not easily detected in the irradiated solutions. The adsorption of phosphate ions onto the surface of the photocatalyst has already been reported.³⁶⁻³⁸ Therefore, a procedure to desorb these compounds was applied (see Section 2 for the correct evaluation of the formation of these ions).

As shown in Fig. 8, photocatalytic treatment of the disulfoton resulted in the destruction of the parent molecule as evidenced by evolution of inorganic anions. Ion chromatography analysis showed the increase of sulfate and phosphate concentration in the reaction mixture as the photocatalysis progressed. The increase indicated that sul-

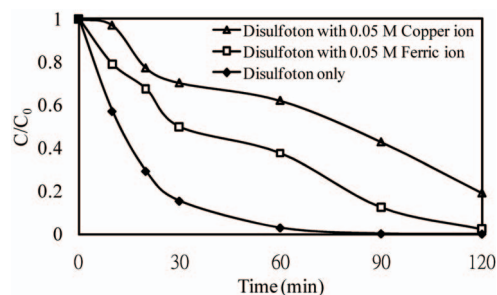


Fig. 7. Effect of cations on the photocatalytic degradation of disulfoton in water. Experimental condition: disulfoton concentration 5 mg L^{-1} , TiO_2 concentration 0.5 g L^{-1} , pH 6.

fur and phosphorus atoms were oxidized to sulfate and phosphate ions, respectively, after they were released from the disulfoton molecule. The stoichiometric concentration of SO_4^{2-} and PO_4^{3-} reached about 95% of the initial organic sulfur and 99% of the initial organic phosphorus in a irradiation time of 6 hours, respectively. The ion chromatographic data confirmed that the complete degradation of disulfoton molecule by photocatalysis led to the conversion of the heteroatoms into inorganic anions.

Separation and identification of the intermediates

After searching the cited literature and to the best of our knowledge, we have come to the conclusion that no prior study has investigated the photocatalytic transformation of disulfoton and very little is known about the use of TiO_2 in the treatment of disulfoton in aqueous solution. In this paper, the photocatalytic degradation mechanism of disulfoton is reported for the first time. Since disulfoton is sparingly soluble in water (water solubility: 12.0 mg L^{-1}), it is therefore a challenge to study its photodegradation in dilute aqueous solutions in the absence of any organic solvents, and to identify its degradation products. A relatively low intensity UV-365 lamp (15W) was used in this study for the identification of organic intermediates. This allowed us to obtain slower degradation rates and provide favorable conditions for the determination of intermediates. Additionally, the initial disulfoton concentration (5 mg L^{-1}) was selected high enough to facilitate the identification of intermediate products.

In photocatalytic degradation process, the concentration of reaction intermediates was low and thus the intermediates had to be preconcentrated before the application of an appropriate analytical procedure. Prior to GC-MS analysis, the samples were preconcentrated using a solid-

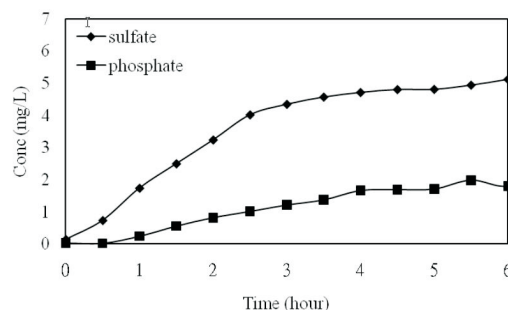


Fig. 8. Evolution of sulfate and phosphate anions originating from disulfoton photocatalytic degradation. Experimental condition: disulfoton concentration 5 mg L^{-1} , TiO_2 concentration 0.5 g L^{-1} , pH 6.

phase microextraction method, a selective tool for the trace analysis of organic compound in water samples. Therefore, the intermediate products generated in the disulfoton solution during the photocatalytic degradation process were analyzed by SPME-GC/MS and identified (a) by using the identification program of NIST library with a fit value higher than 70%, (b) by comparing the spectra with previously reported spectra and (c) by the interpretation of the mass spectra and the investigation of their characteristic ions.

Fig. 9 displays the chromatogram of the reacted solution after irradiation for 20 min. At least eight components were identified at retention times less than 40 min. One of the peaks was the initial disulfoton (peak I); the other seven (new) peaks were the intermediates formed. The disulfoton and its related intermediates were denoted as species I–VIII. Except for the initial disulfoton, the other peaks increased at first and subsequently decreased, indicating the formation and subsequent transformation of the intermediates. Table 3 summarizes the identified intermediates of disulfoton along with their retention time and the characteristic ions of the mass spectra. Some other minor peaks were presented, but mass fragment information did not allow elucidation of their structures.

The molecular mass of these compounds was determined using positive ion chemical ionization (CI) mass spectrometry through the abundant protonated molecule $[M+H]^+$, and the structural data were obtained from the electron impact (EI) fragmentation patterns. Five intermediates (III, V–VIII) were identified by the molecular ion and mass fragment ions and also through the comparisons with NIST library data. The similarities of these compounds to

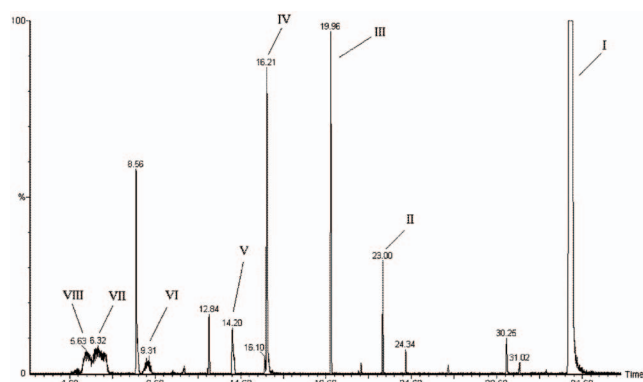


Fig. 9. GC/MS chromatogram obtained for disulfoton solution after 20 min of irradiation with UV light in the presence of TiO_2 .

Table 3. Identification of the intermediates from the photocatalytic degradation of disulfoton by GC/MS

Structure	t_R (min)	Characteristic ions (m/z)
	34.04	$[M]^+$ = 65, 88, 97, 125, 142, 153, 186, 274 (I) Disulfoton
	23.00	$[M]^+$ = 47, 65, 97, 125, 153, 186, 214 (II) Dithiophosphoric acid-O,S,O-triethylester
	19.96	$[M]^+$ = 47, 61, 75, 89, 150 (III) 1,2-Bis(ethylthio)ethane
	16.21	$[M]^+$ = 47, 61, 75, 122 (IV) 2-(Ethylthio)ethanethiol
	14.20	$[M]^+$ = 29, 66, 94, 122 (V) 1,2-Diethyldisulfane
	9.31	$[M]^+$ = 47, 61, 88 (VI) Ethyl(vinyl)sulfane
	6.32	$[M]^+$ = 29, 47, 62 (VII) Ethanethiol
	5.63	$[M]^+$ = 31, 45 (VIII) Ethanol

the NIST library data were more than 72%. Two intermediates (II and IV) not included in the library were identified by the molecular ion and the interpretation of the mass spectra.

Fig. 1S shows the EI mass spectra of intermediates formed during the photocatalytic degradation of disulfoton in the presence of TiO_2 (0.5 g L^{-1}) particles. The molecular mass of compound II was determined from the EI mass spectrum to be $m/z = 214$, which was confirmed by the observation of an $[M+H]^+$ ion of 215 using positive ion CI mass spectrometry (Fig. 2S). The EI mass spectrum showed the characteristic ions at $m/z = 153$, $m/z = 125$ and $m/z = 97$ corresponding to the groups, $[(C_2H_5O)_2P(S)]^+$, $[(C_2H_5O)P(S)(OH)]^+$ and $[(HO)_2P(S)]^+$, respectively. Based on these data, compound II was identified as dithiophosphoric acid-O,S,O-triethylester. Zamy et al.²⁴ investigated the analysis of disulfoton aqueous solutions after irradiation ($\lambda > 285 \text{ nm}$) and showed the formation of dithiophosphoric acid-O,S,O-triethylester.

The molecular mass of compound III was determined from the CI mass spectrum to be $m/z = 150$ by the observation of an $[M+H]^+$ ion of 151 (Fig. 3S). A search of the EI mass spectra library selected 1, 2-bis(ethylthio)ethane as a good match (98%) for compound III. It exhibited the characteristic ions at $m/z = 89$, $m/z = 75$, and $m/z = 61$ corre-

sponding to the groups [CH₂CH₂SCH₂CH₃]⁺, [CH₂=SCH₂CH₃]⁺ and [CH₃CH₂S]⁺, respectively. This compound was also identified, in a previous study, as a by-product of disulfoton hydrolysis.³⁹

The molecular mass of compound **IV** was determined from the CI mass spectrum to be $m/z = 122$ by the observation of an [M+H]⁺ ion of 123 (Fig. 4S). The EI mass spectrum showed the characteristic ions at $m/z = 75$, $m/z = 61$ and $m/z = 47$ corresponding to the groups, [CH₂=SCH₂CH₃]⁺, [HSCH₂CH₂]⁺ and [HS=CH₂]⁺, respectively. Based on these data, compound **IV** was identified as 2-(ethylthio)ethanethiol.

Compound **V** was identified as 1,2-diethyldisulfane by a library search with a fit value of 93%. This intermediate was confirmed by the comparison of MS spectrum and GC retention time with an authentic compound obtained from Aldrich Chemical Co. Neat 1,2-diethyldisulfane, dissolved in methanol, yielded the same GC retention time and mass spectrum as that of the suspected 1,2-diethyldisulfane found in the irradiated samples of disulfoton photocatalytic experiment. 1,2-Diethyldisulfane is an interesting intermediate because it is most likely to form from the dimerization of ethanethiol (a molecular segment of disulfoton's side chain).

The mass spectrum of compound **VI** exhibited a peak at $m/z = 88$ which corresponded to the molecular ion [M]⁺. A search of the mass spectra library revealed ethyl(vinyl)sulfane to be a good match (90%) for compound **VI**, the retention time of which on GC was 9.31 min.

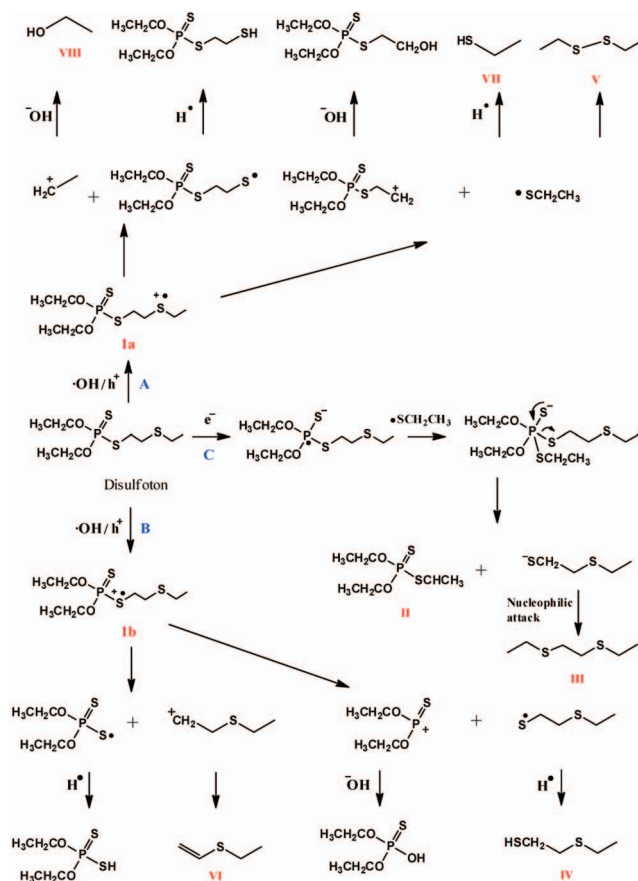
Compound **VII** was identified as ethanethiol by a library search with a fit value of 72%. The mass spectrum of this compound showed a peak at $m/z = 62$ which corresponded to the molecular ion [M]⁺, and the characteristic ion at $m/z = 47$ corresponding to the group [CH₂=SH]⁺.

Compound **VIII** was identified as ethanol with a fit value of 92% found by searching the mass spectra library. This compound was further identified by matching its retention time and mass spectrum with that of an authentic standard. They exhibited the exact retention time and similar mass spectra.

Initial photooxidation pathway

Scheme I shows the proposed mechanism for the generation of the primary detected intermediates. Oxidation of the disulfoton molecule to form the disulfoton cation radical took place when positive holes attacked it, initiating a series of reactions. The formation of cation radicals were also observed in the photocatalytic degradation of other

Scheme I Proposed photodegradation pathway of disulfoton under UV irradiation in aqueous TiO₂ dispersions



organophosphorus pesticides.^{15,40-42}

In path A, the interfacial transfer of a single electron from the sulfur atom, which was located far from the phosphorus atom, led to the formation of disulfoton cation radical **1a** (Scheme I, path A). The scission of the C-S bond in the cation radical **1a** led to the formation of [•]SC₂H₅ radicals which were the precursor of ethanethiol (compound **VII**). The H atoms necessary for S-H bond formation were proposed to be originated from the proton reduction by photo-generated electrons H⁺ + e⁻ → H[•] as already observed in the degradation of the insecticide fenitrothion by Kerzhentsev et al.⁴³ The recombination of [•]SC₂H₅ radicals could form dimers such as 1,2-diethyldisulfane (compound **V**). The dimerization of thiol radical was also reported in the case of the photocatalytic degradation of thiocarbamate pesticides.¹⁷ Similarly, the scission of the C-S bond in the cation radical **1a** led to the formation of ethanium cation [CH₃CH₂]⁺. This carbocation was extremely unstable and

underwent rapid hydrolysis to yield ethanol (compound **VIII**).

The interfacial transfer of a single electron from the sulfur atom, located near the phosphorus atom, led to the formation of disulfoton cation radical **1b** (Scheme I, path B). The scission of the C-S bond in this cation radical led to the formation of $(C_2H_5O)_2P(S)S^{\bullet}$ radicals and 2-(ethylthio)ethan-1-ylum ions. The carbocation was extremely unstable and underwent rapid hydrolysis and dehydrogenation. Hydrolysis of this carbocation yielded 2-(ethylthio)ethanol while the dehydrogenation led to the formation of ethyl(vinyl)sulfane (compound **VI**). Additionally, the scission of the P-S bond in the disulfoton cation radical **1b** led to the formation of 2-(ethylthio)ethanethiol (compound **IV**).

In path C, dithiophosphoric acid-O,S,O-triethylester (compound **II**) and 2-(ethylthio)ethanethiolate were formed by electron transfer followed by $\bullet SC_2H_5$ radical addition-elimination reaction.⁴⁰ 2-(ethylthio)ethanethiolate was the precursor of 1,2-bis(ethylthio)ethane (compound **III**), which acted as the nucleophile and attacked disulfoton at α -carbon of ethoxy group. The thiophosphate esters might react like alkyl halides by nucleophilic displacement at the carbon bound to the oxygen of an alcohol moiety.⁴⁴

Relative photonic efficiency and quantum yield

Quantum yield is an important parameter in photochemistry. Its precise measurement is often difficult in a heterogeneous dispersion owing to non-negligible scattering of the light irradiance impinging on the reactor.⁴⁵ Considering the difficulty of quantum yield measurements, phenol was selected as a standard secondary actinometer to assess the relative photonic efficiency (ξ_{rel}) of the photodegradation of disulfoton against phenol according to the protocol reported by Serpone et al..⁴⁶

$$\xi_{rel} = \frac{\text{rate of disappearance of substrate}}{\text{rate of disappearance of phenol}} \quad (7)$$

In this study, the relative photonic efficiency ξ_{rel} was 2.43 determined under identical experimental conditions (initial concentration of reactant, 0.0182 mM [100 mL]; TiO_2 loading, 0.5 g L⁻¹ [P25]; pH 6). The quantum yield could subsequently be determined from ξ_{rel} , as $\Phi_{disulfoton} = \xi_{rel}\Phi_{phenol}$, where Φ_{phenol} was the quantum yield for the photocatalyzed oxidative degradation of phenol using Degussa P25 TiO_2 as the standard catalyst material. The quantum yield of photodegradation of phenol was determined ($\Phi_{phenol} = 0.11 \pm 0.01$) by Serpone et al..⁴⁷ Therefore,

actinometer studies resulted in a reaction quantum yield for disulfoton of 0.267.

Electrical energy efficiency

UV/ TiO_2 photodegradation of aqueous organic pollutant is an electric-energy intensive process, and electric energy can represent a major fraction of the operating costs, simple figure-of-merit based on electric energy consumption can be very useful. In the case of low pollutant concentrations, the appropriate figure-of-merit was the *electrical energy per order* (E_{EO}), defined as the number of kilowatt hours of electrical energy required to reduce the concentration of a pollutant by one order of magnitude (90%) in 1 m³ of contaminated water. The E_{EO} (kWh/(m³ order)) could be calculated from the following equations:⁴⁸

$$E_{EO} = \frac{P \times t \times 1000}{V \times 60 \times \log(C_0 / C)} \quad (8)$$

$$E_{EO} = \frac{38.4 \times P}{V \times k_{app}} \quad (9)$$

where P is the power input (kW) from the wall to drive the UV lamp, t is the irradiation time (min), V is the volume (L) of the water in the reactor, C_0 and C are the initial and final pollutant concentrations, and k_{app} is the pseudo-first-order rate constant (min⁻¹) for the decay of the pollutant concentration. The degradation of disulfoton was found to follow pseudo-first-order kinetics, and hence the figure-of-merit electrical energy per order (E_{EO}) was appropriate for estimating the electrical energy efficiency. This study showed that disulfoton could be treated easily and effectively with the TiO_2/UV process with E_{EO} value of 85 kWh/(m³ order).

CONCLUSION

Disulfoton could be successfully degraded by TiO_2 under UV irradiation for 90 min and ca. 99% of disulfoton was degraded. The photodegradation rate of disulfoton was found to increase along with increasing pH and to increase, and then decrease along with increasing catalyst concentration. In addition, the presence of inorganic ions such as Cl^- and NO_3^- that were often presented in natural water systems decreased the photocatalytic degradation rate of disulfoton.

Establishment of the reaction pathway was made possible by a thorough analysis of the reaction mixture identifying the main intermediate products generated. Eight intermediates were identified and characterized

through a mass spectra analysis. The reaction pathway could proceed via the formation of disulfoton cation radicals by attacking positive holes to initiate the series of reactions. The interfacial transfer of a single electron from the sulfur atom initiated C-S bond cleavage and led to the formation of the detected intermediates. Another reaction pathway might involve in electron transfer to central P atom of disulfoton followed by $\cdot\text{SC}_2\text{H}_5$ radical addition-elimination reaction.

The relative photonic efficiency for the photodegradation of disulfoton was estimated against phenol as the secondary standard. Actinometer studies resulted in a reaction quantum yield for disulfoton of 0.267. The degradation of disulfoton was found to follow pseudo-first-order kinetics, and hence the figure-of-merit electrical energy per order (E_{EO}) was appropriate for estimating the electrical energy efficiency. This study showed that disulfoton could be treated easily and effectively with the TiO₂/UV process with E_{EO} value of 85 kWh/(m³ order).

ACKNOWLEDGMENTS

This work was supported by NSC 99-2113-M-025-001-MY2 of the National Science Council of the Republic of China.

REFERENCES

- Schimmel, S. C.; Garnas, R. L.; Patrick, J.-M.; Moore, J. C. *J. Agric. Food Chem.* **1983**, *31*, 104.
- Racke, K.-D. *Organophosphates: Chemistry, Fate, and Effects*; San Diego: Academic Press, 1992; pp 48-78.
- Arnold, H.; Pluta, H.-J.; Braunbeck, T. *Aquat. Toxicol.* **1995**, *33*, 17.
- Raushel, F. M. *Curr. Opin. Microbiol.* **2002**, *5*, 288.
- Sogorb, M. A.; Vilanova, E. *Toxicol. Lett.* **2002**, *128*, 215.
- Jokanović, M. *Toxicology* **2001**, *166*, 139.
- Juarez, S. L. M.; Sanchez, J. *Bull. Environ. Contam. Toxicol.* **1989**, *43*, 302.
- Gan, Q.; Jans, U. *J. Agric. Food Chem.* **2006**, *54*, 7753.
- Foo, K. Y.; Hameed, B. H. *J. Hazard. Mater.* **2010**, *175*, 1.
- Mascolo, G.; Lopez, A.; Foldenyi, R.; Passino, R.; Tiravanti, G. *Environ. Sci. Technol.* **1995**, *29*, 2987.
- Lacorte, S.; Lartiges, S. B.; Garrigues, P.; Barcelo, D. *Environ. Sci. Technol.* **1995**, *29*, 431.
- Somich, C. J.; Muldoon, M. T.; Kearney, P. C. *Environ. Sci. Technol.* **1990**, *24*, 745.
- Islam, M. A.; Sakkas, V.; Albanis, T. A. *J. Hazard. Mater.* **2009**, *170*, 230.
- Akhtar, M.; Hasany, S. M.; Bhangar, M. I.; Iqbal, S. *Chemosphere* **2007**, *66*, 1829.
- Konstantinou, I. K.; Sakellarides, T. M.; Sakkas, V. A.; Albanis, T. A. *Environ. Sci. Technol.* **2001**, *35*, 398.
- Kearney, P. C.; Muldoon, M. T.; Somich, C. J.; Ruth, J. M.; Voden, D. J. *J. Agric. Food Chem.* **1988**, *36*, 1301.
- Vidal, A.; Dinya, Z.; Jr, F. M.; Mogyorodi, F. *Appl. Catal. B: Environ.* **1999**, *21*, 259.
- Kim, T. S.; Kim, J. K.; Choi, K.; Stenstrom, M. K.; Zoh, K.-D. *Chemosphere* **2006**, *62*, 926.
- Wu, R. J.; Chen, C. C.; Lu, C. S.; Hsu, P. Y.; Chen, M. H. *Desalination* **2010**, *250*, 869.
- Pellzzetti, E.; Maurino, V.; Minero, C.; Carlin, V.; Pramauro, E.; Zerbini, O.; Tosato, M. *Environ. Sci. Technol.* **1990**, *24*, 1559.
- Konstantinou, I. K.; Albanis, T. A. *Appl. Catal. B: Environ.* **2003**, *42*, 319.
- Hoffmann, M. R.; Martin, S. T.; Choi, W.; Bahnemann, D. W. *Chem. Rev.* **1995**, *95*, 69.
- Wu, T.; Liu, G.; Zhao, J.; Hidaka, H.; Serpone, N. *J. Phys. Chem. B* **1999**, *103*, 4862.
- Zamy, C.; Mazellier, P.; Legube, B. *Wat. Res.* **2004**, *38*, 2305.
- Hebert, V. R.; Miller, G. C. *J. Agric. Food Chem.* **1990**, *38*, 913.
- Wu, R. J.; Chen, C. C.; Chen, M. H.; Lu, C. S. *J. Hazard. Mater.* **2009**, *162*, 945.
- Zhu, X.; Yuan, C.; Bao, Y.; Yang, J.; Wu, Y. *J. Mol. Catal. A: Chem.* **2005**, *229*, 95.
- Chu, W.; Wong, C. C. *Wat. Res.* **2004**, *38*, 1037.
- Konstantinou, I. K.; Sakkas, V. A.; Albanis, T. A. *Wat. Res.* **2002**, *36*, 2733.
- Chu, W.; Rao, Y.; Hui, W. Y. *J. Agric. Food Chem.* **2009**, *57*, 6944.
- Wu, C. H.; Chern, J. M. *Ind. Eng. Chem. Res.* **2006**, *45*, 6450.
- Liang, H. C.; Li, X. Z.; Yang, Y. H.; Sze, K. H. *Chemosphere* **2008**, *73*, 805.
- Sökmen, M.; Ozkan, A. *J. Photochem. Photobiol. A: Chem.* **2002**, *147*, 77.
- Mahmoodi, N. M.; Arami, M.; Limaee, N. Y.; Gharanjig, K. *J. Hazard. Mater.* **2007**, *145*, 65.
- Surolia, P. K.; Tayade, R. J.; Jasra, R. V. *Ind. Eng. Chem. Res.* **2007**, *46*, 6196.
- Echavia, G. R. M.; Matzusawa, F.; Negishi, N. *Chemosphere* **2009**, *76*, 595.
- Abdullah, M.; Low, G. K.-C.; Matthews, R. W. *J. Phys. Chem.* **1990**, *94*, 6820.
- Hermann, J. M.; Guillard, C.; Arguello, M.; Agüera, A.; Tejedor, A.; Piedra, L.; Fernández-Alba, A. *Catal. Today* **1999**, *54*, 353.
- Dannenberg, A.; Pehkonen, S. O. *J. Agric. Food Chem.* **1998**, *46*, 325.

40. Evgenidou, E.; Konstantinou, I.; Fytianos, K.; Albanis, T. *J. Hazard. Mater. B* **2006**, *137*, 1056.
41. Konstantinou, I. K.; Sakkas, V. A.; Albanis, T. A. *Appl. Catal. B: Environ.* **2001**, *34*, 227.
42. Fox, M. A.; Abdel-Wahad, A. A. *Tetrahedron Lett.* **1990**, *31*, 4533.
43. Kerzhentsev, M.; Guillard, C.; Herrmann, J. M.; Pichat, P. *Catal. Today* **1996**, *27*, 215.
44. Gan, Q.; Jans, U. *J. Agric. Food Chem.* **2007**, *55*, 3546.
45. Augugliaro, V.; Loddo, V.; Palmisano, L.; Schiavello, M. *J. Catal.* **1995**, *153*, 32.
46. Serpone, N.; Sauvé, G.; Koch, R.; Tahiri, H.; Pichat, P.; Piccinini, P.; Pelizzetti, E.; Hidaka, H. *J. Photochem. Photobiol. A: Chem.* **1996**, *94*, 191.
47. Serpone, N. *J. Photochem. Photobiol. A: Chem.* **1997**, *104*, 1.
48. Salari, D.; Daneshvar, N.; Aghazadeh, F.; Khataee, A. R. *J. Hazard. Mater. B* **2005**, *125*, 205.